Hindawi Publishing Corporation
Journal of Control Science and Engineering
Volume 2008, Article ID 491625, 11 pages
doi:10.1155/2008/491625

Research Article

Nonlinear Speed Control of Switched Reluctance Motor Drives Taking into Account Mutual Inductance

M. Alrifai,[1] M. Zribi,[1] R. Krishnan,[2] and M. Rayan[1]

[1] *Electrical Engineering Department, College of Engineering and Petroleum, Kuwait University, P.O. Box 5969, Safat 13060, Kuwait*
[2] *Center for Rapid Transit Systems, Electrical and Computer Engineering Department, Virginia Tech University, 461 Durham Hall, Blacksburg, VA 24061-011, USA*

Correspondence should be addressed to M. Alrifai, alrifm@eng.kuniv.edu.kw

Received 4 November 2007; Accepted 28 December 2007

Recommended by Benoit Boulet

A speed control algorithm is proposed for variable speed switched reluctance motor (SRM) drives taking into account the effects of mutual inductances. The control scheme adopts two-phase excitation; exciting two adjacent phases can overcome the problems associated with single-phase excitation such as large torque ripple, increased acoustic noise, and rotor shaft fatigues. The effects of mutual coupling between two adjacent phases and their contribution to the generated electromagnetic torque are considered in the design of the proposed control scheme for the motor. The proposed controller guarantees the convergence of the currents and the rotor speed of the motor to their desired values. Simulation results are given to illustrate the developed theory; the simulation studies show that the proposed controller works well. Moreover, the simulation results indicate that the proposed controller is robust to changes in the parameters of the motor and to changes in the load torque.

1. INTRODUCTION

Switched reluctance motors (SRMs) have gained increasing popularity in recent years due to their simplicity of construction, low cost, and simplicity of the associated unipolar power converters. Moreover, SRMs can produce high torque at low speeds. These characteristics, combined with advanced power electronic devices, and the availability of high-speed processors make these motors attractive for many applications not only for low performance applications such as fans and hand-tools but also for high dynamic performance applications such as electric vehicles and motors used for aerospace applications.

The switched reluctance motor is a doubly salient brushless motor, with concentrated copper windings on the stator poles, and no windings or magnets on the rotor poles. Both stator and rotor cores are constructed from iron laminations. Each phase is wound on diametrically opposite stator poles. Figure 1 shows the cross-section of an SRM with eight stator poles and six rotor poles (a typical 8/6 SRM). Excitation of a phase, that is, excitation of a pair of diametrically opposite stator poles, causes the nearest pair of rotor poles to align with the excited stator poles. This produces torque regardless of the direction of the current in the phase winding. Therefore, only unipolar currents are required in stator phases, and sequential excitation based on rotor position causes the rotor to rotate and align its poles with the excited stator poles. A shaft position encoder is often used to provide the rotor position information. The reader can refer to [1–3] and the references therein for more details on SRMs.

Both spatial and magnetic nonlinearities are inherent characteristics of the SRM. As a result, the dynamic equations of the SRM are nonlinear and time varying. High performance can hardly be achieved by using conventional linear controllers because linearizing the system dynamics around an operating point and designing a linear controller is generally not sufficient to achieve the high dynamical performance required for high performance drives. Therefore, it is necessary to take the system nonlinearities into account and design feedback control laws that compensate for the system nonlinearities and parameter uncertainties.

Many researchers have focused on the control of switched reluctance motors. Optimal current profiling [4] and torque distribution functions [5–9] were proposed in the literature to minimize torque ripples during commutation. In [5, 6], the basic idea was to distribute the desired torque

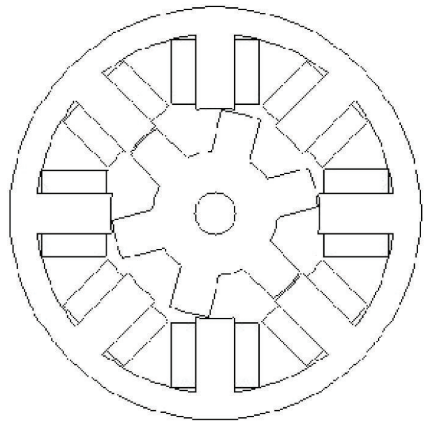

Figure 1: The cross-section of an 8/6 SRM.

to two adjacent phases during commutation using proposed torque distribution functions. Linearly decreasing the outgoing phase and increasing the incoming phase during the commutation interval was proposed in [7] to obtain a high performance torque controller. In [8], a torque distribution function that minimizes the rates of change of currents over the commutation interval was proposed. In some of these control schemes, an ideal inductance profile was assumed. However, none of these controllers considered the effects of mutual inductances during commutation. The effects of mutual inductance and the possibility of two-phase excitation were mentioned in [9–14], but no active control scheme was suggested to overcome the effects of mutual inductances. A novel dynamic model for the SRM which is suitable for two-phase excitation control studies and which takes into account the mutual inductance was proposed in [15]. In that paper, a torque distribution function which reduces the rates of change of currents and which compensates for the effects of mutual coupling was presented; a control scheme which is based on linearizing and decoupling the SRM model was also proposed.

Due to the developments in nonlinear control theory, many nonlinear control techniques have been developed for nonlinear systems in the last three decades or so. Among these techniques are feedback linearization control, sliding mode control, adaptive control, optimal control neural control, fuzzy logic control, and backstepping control. Although some of these nonlinear control techniques have been known for some time now, it is only recently that they are being applied to SRM drives.

Some of the speed controllers for the SRM reported in the literature are open loop in nature. These controllers do not achieve high dynamic performance which rivals that of DC and AC motor-based drives. The main purpose of this research is to investigate the development of a nonlinear control scheme that can achieve high dynamical performance as required for speed regulation of an SRM while taking into account mutual inductances.

In this paper, a nonlinear speed controller is proposed for the SRM drive. The mathematical model proposed in [15] for the SRM is adopted. The adopted model is suitable for two-phase excitation and takes into account the effects of mutual inductance between two adjacent phases. Simulation results indicate that the proposed controller works well and it is robust to changes in the parameters of the system and to changes in the load torque.

The paper is organized as follows. The model of the SRM which takes into account mutual inductance is presented in Section 2. In Section 3, a nonlinear feedback controller is proposed for the SRM. Simulation results are presented and discussed in Section 4. Finally, some concluding remarks are given in Section 5.

2. MODELING OF THE SWITCHED RELUCTANCE MOTOR INCLUDING MUTUAL INDUCTANCE

Using a reliable mathematical model is essential for properly evaluating the SRM performances when different control schemes are used. Both spatial and magnetic nonlinearities are inherent characteristics of the SRM and, as a result the motor parameters, are functions of the rotor position and current. The model introduced by [15], which takes into account mutual inductance, is adopted in this paper. In many linear drive applications [16, 17], the SRM is operating in the magnetically linear region where the parameters of the system are expressed as functions of the rotor position only. In this paper, magnetic saturation is not considered and the analysis of the SRM is performed assuming that the motor operates in the linear magnetic region. The extension of the proposed control algorithm to include the nonlinear operation region can be achieved by expressing the inductances in terms of the rotor position and the phase currents.

2.1. The parameters of the SRM

The parameters of the SRM, such as self-inductances, mutual inductances, and the rates of change of the inductances with respect to the rotor position, are usually obtained analytically by the finite element analysis (FEA) method and they are usually verified experimentally by measurements [18–24]. The SRM parameters obtained by the FEA method and experimentally verified in [15] are adopted in this paper; some small changes due to curve fitting are made. The SRM used is operating in the linear magnetic region when the load torque is less than 0.2 Nm or when the phase current is less than 1.2 amp. Therefore, motor parameters are obtained at phase currents equal to 1.2 amp.

The rates of change of the self- and mutual inductances, with respect to rotor position, are defined as the self-torque functions and the mutual torque functions, respectively. They are denoted as follows:

$$g_k(\theta) = \frac{\partial L_k(\theta)}{\partial \theta} \quad \text{for } k = a, b, c, d,$$
$$g_{jk}(\theta) = \frac{\partial M_{jk}(\theta)}{\partial \theta} \quad \text{for } jk = ab, bc, cd, da, \tag{1}$$

where L_k is the phase inductance of phase k, M_{jk} is the

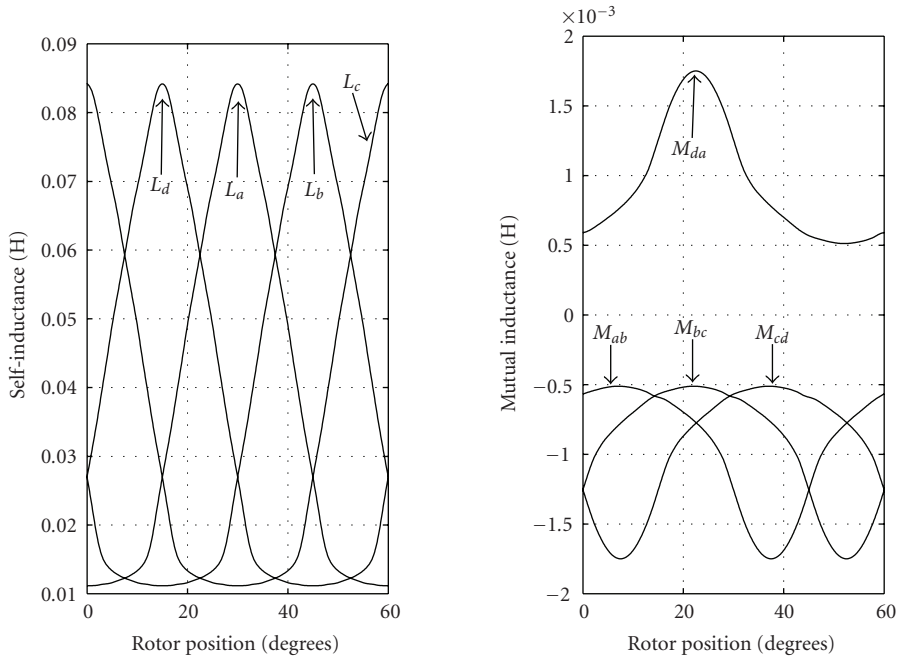

Figure 2: The self- and mutual inductances of the used 8/6 SRM.

mutual inductance between phase j and phase k, and θ is the rotor position.

The self-inductances and the mutual inductances of the prototype SRM are shown in Figure 2. From the geometry of the prototype SRM with 8 stator and 6 rotor poles, it is noticed that all the parameters have a period of 60° and there is a phase shift of 15° between adjacent phases. The mutual inductance between the two adjacent phases is not greater than 6.4% of the related self-inductances at any position. The mutual inductance between the two nonadjacent phases is negligible as they are less than 0.07% of the self-inductances.

By examining the properties of the self-torque functions and the torque functions from the plots in Figure 2, it can be deduced that two adjacent phases can generate the desired output torque during a period of 15° degrees because the polarities of the self-torque functions are equal during that interval. This interval is defined as the excitation region. There are four different excitation region in a period and only two phases are useful in an excitation region. In addition, it is noticed that the mutual coupling between them is not negligible [15]. In Figures 3 and 4, the considered torque functions in each region are redrawn from Figure 2. The mutual torque functions are magnified ten times for ease of comparison. The waveforms of the corresponding self-torque functions in four regions at the same torque are equal. However, the waveforms of the mutual torque functions in the first region when T_e is positive and the third region when T_e is negative are different from the waveforms of the mutual torque functions in other excitation regions because only the mutual coupling between phases d and a is additive.

2.2. Dynamic equations for two-phase excitation of the SRM

To include the effects of mutual coupling, two phases are considered simultaneously. A four-phase system can be considered as a two-phase system because only one excitation region is considered at one time. Thus, the four phases equations are reduced to two-phase equations as proposed in [15], and they are written as follows:

$$\begin{aligned}
\frac{di_x}{dt} &= -a_1 i_x - a_2 \omega i_x + a_3 i_y + a_4 \omega i_y + a_0 \left(v_x - \frac{M_{xy}}{L_y} v_y \right), \\
\frac{di_y}{dt} &= -b_1 i_y - b_2 \omega i_y + b_3 i_x + b_4 \omega i_x + b_0 \left(v_y - \frac{M_{xy}}{L_x} v_x \right), \\
\frac{d\omega}{dt} &= -\frac{B}{J}\omega + \frac{1}{J} T_e
\end{aligned} \tag{2}$$

with

$$T_e = \frac{1}{2} g_x i_x^2 + \frac{1}{2} g_y i_y^2 + g_{xy} i_x i_y = c_2 J i_x^2 + c_3 J i_y^2 + c_4 J i_x i_y, \tag{3}$$

where the subscript x and y are the phases in consideration and the set (x, y) is one of (a, b), (b, c), (c, d), and (d, a). Either phase x or phase y is leading and the other phase is following according to the direction of rotation. The phase voltages for phase x and phase y are denoted as v_x and v_y, respectively. The phase currents in phase x and phase y are denoted as i_x and i_y, respectively. The speed of the rotor is denoted as ω, θ is the rotor position, J is the rotor inertia, B is the damping factor, and T_e is the motor torque.

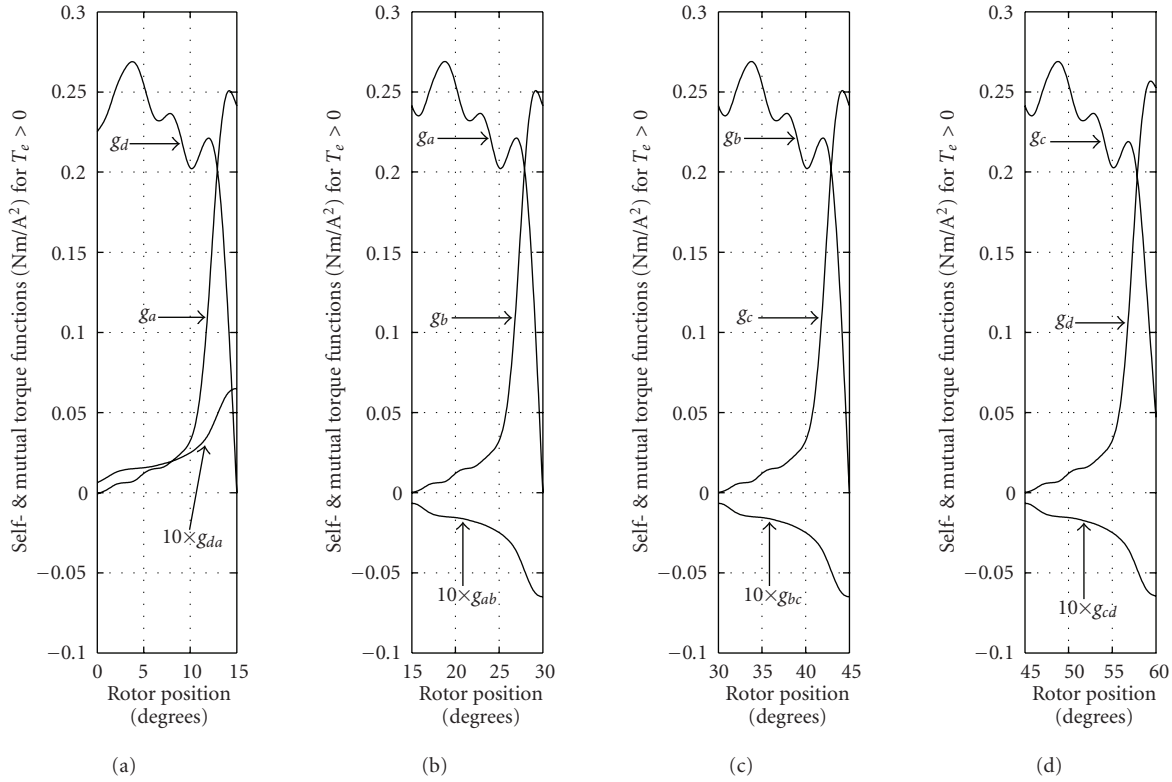

Figure 3: The self- and mutual torque functions for positive torque.

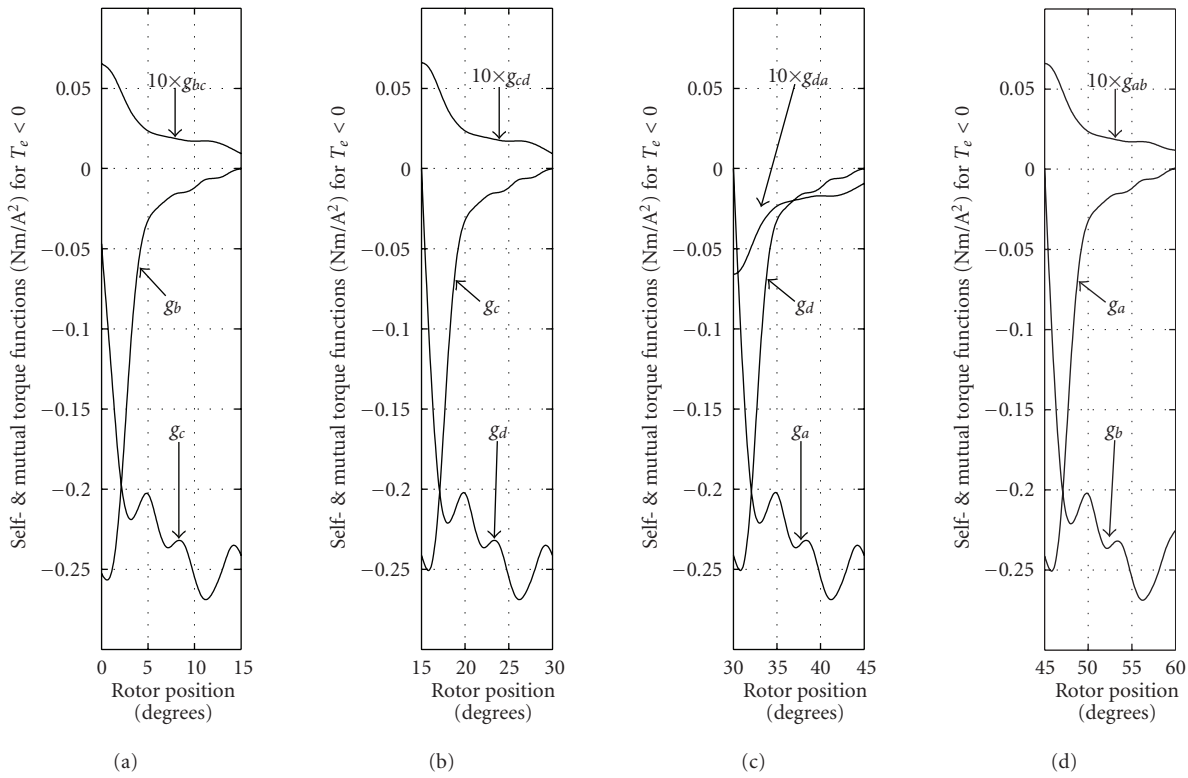

Figure 4: The self- and mutual torque functions for negative torque.

The parameters of the motor are such that

$$
\begin{aligned}
c_1 &= \frac{B}{J}, \qquad c_2 = \frac{1}{2J}g_x,\\
c_3 &= \frac{1}{2J}g_y, \qquad c_4 = \frac{1}{J}g_{xy},\\
D &= L_xL_y - M_{xy}^2,\\
a_0 &= \frac{1}{D}L_y, \qquad a_1 = a_0R_s,\\
a_2 &= a_0\left(g_x - \frac{M_{xy}}{L_y}g_{xy}\right), \qquad a_3 = a_0\frac{M_{xy}R_s}{L_y},\\
a_4 &= a_0\left(-g_{xy} + \frac{M_{xy}}{L_y}g_y\right),\\
b_0 &= \frac{1}{D}L_x, \qquad b_1 = b_0R_s,\\
b_2 &= b_0\left(g_y - \frac{M_{xy}}{L_x}g_{xy}\right), \qquad b_3 = b_0\frac{M_{xy}R_s}{L_x},\\
b_4 &= b_0\left(-g_{xy} + \frac{M_{xy}}{L_x}g_x\right),
\end{aligned}
\tag{4}
$$

where R_s is the winding phase resistance. It should be mentioned that most of the motor parameters are implicitly dependent on θ since $d\theta/dt = \omega$.

Let u_x and u_y be such that

$$
\begin{aligned}
u_x &= v_x - \frac{M_{xy}}{L_y}v_y,\\
u_y &= v_y - \frac{M_{xy}}{L_x}v_x.
\end{aligned}
\tag{5}
$$

Note that using u_x and u_y, given in (5), one can obtain the phase voltages v_x and v_y such that

$$
\begin{aligned}
v_x &= \frac{L_xL_y}{D}u_x + \frac{L_xM_{xy}}{D}u_y,\\
v_y &= \frac{L_yM_{xy}}{D}u_x + \frac{L_xL_y}{D}u_y.
\end{aligned}
\tag{6}
$$

Also let the state variables x_1, x_2, and x_3 be such that $x_1 = i_x$, $x_2 = i_y$, and $x_3 = \omega$. Then, the model of the SRM motor, given by (2) and (3), can be written as

$$
\begin{aligned}
\dot{x}_1 &= -a_1x_1 - a_2x_3x_1 + a_3x_2 + a_4x_3x_2 + a_0u_x,\\
\dot{x}_2 &= -b_1x_2 - b_2x_3x_2 + b_3x_1 + b_4x_3x_1 + b_0u_y,\\
\dot{x}_3 &= -c_1x_3 + c_2x_1^2 + c_3x_2^2 + c_4x_1x_2.
\end{aligned}
\tag{7}
$$

The objective of the paper is to design a control scheme such that the motor speed is driven to a desired constant speed ω_d.

Define i_{xd}, i_{yd}, and ω_d as the desired values of the phase currents i_x, i_y and the speed ω, respectively. Note that ω_d is constant.

The motor torque T_e, expressed by (3), can be indirectly controlled to a desired value by controlling phase currents. Torque distribution functions which reduce the rate of change of phase currents and compensate for the mutual coupling were proposed in [15]. In that paper, the authors suggested an approach to calculate the desired phase currents using self- and mutual torque functions given by (1), this approach is adopted in this paper and the equations used to calculate the desired phase currents are as follows:

$$
\begin{aligned}
i_{xd} &= \sqrt{\frac{2g_xT_e}{g_x^2 + g_y^2 \pm 2g_{xy}\sqrt{g_xg_y}}},\\
i_{yd} &= \sqrt{\frac{2g_yT_e}{g_x^2 + g_y^2 \pm 2g_{xy}\sqrt{g_xg_y}}}.
\end{aligned}
\tag{8}
$$

Note that in (8), the "$\pm$" term should be interpreted as follows: a plus sign is used when the desired output torque T_e is positive and minus sign is used when T_e is negative.

It should be noted that the desired values should satisfy the equation

$$
-c_1\omega_d + c_2i_{xd}^2 + c_3i_{yd}^2 + c_4i_{xd}i_{yd} = 0. \tag{9}
$$

Equation (9) can be easily obtained from the dynamic model given in (7).

Define the following errors:

$$
\begin{aligned}
e_1(t) &= x_1(t) - i_{xd}(t),\\
e_2(t) &= x_2(t) - i_{yd}(t),\\
e_3(t) &= x_3(t) - \omega_d.
\end{aligned}
\tag{10}
$$

Hence, using (7), (9), and (10), the model of the SRM motor can be written as

$$
\begin{aligned}
\dot{e}_1 &= -a_1(e_1 + i_{xd}) - a_2(e_3 + \omega_d)(e_1 + i_{xd}) + a_3(e_2 + i_{yd})\\
&\quad + a_4(e_3 + \omega_d)(e_2 + i_{yd}) - di_{xd} + a_0u_x,\\
\dot{e}_2 &= -b_1(e_2 + i_{yd}) - b_2(e_3 + \omega_d)(e_2 + i_{yd}) + b_3(e_1 + i_{xd})\\
&\quad + b_4(e_3 + \omega_d)(e_1 + i_{xd}) - di_{yd} + b_0u_y,\\
\dot{e}_3 &= -c_1(e_3 + \omega_d) + c_2(e_1 + i_{xd})^2 + c_3(e_2 + i_{yd})^2\\
&\quad + c_4(e_1 + i_{xd})(e_2 + i_{yd})
\end{aligned}
\tag{11}
$$

with $di_{xd} = di_{xd}/dt$, $di_{yd} = di_{yd}/dt$, and $d\omega_d/dt = 0$, or

$$\begin{aligned}
\dot{e}_1 &= -a_1 e_1 - a_1 i_{xd} - a_2 e_1 e_3 - a_2 i_{xd} e_3 - a_2 \omega_d e_1 \\
&\quad - a_2 i_{xd} \omega_d + a_3 e_2 + a_3 i_{yd} + a_4 e_2 e_3 + a_4 i_{yd} e_3 \\
&\quad + a_4 \omega_d e_2 + a_4 i_{yd} \omega_d - di_{xd} + a_0 u_x \\
\dot{e}_2 &= -b_1 e_2 - b_1 i_{yd} - b_2 e_2 e_3 - b_2 i_{yd} e_3 - b_2 \omega_d e_2 \\
&\quad - b_2 i_{yd} \omega_d + b_3 e_1 + b_3 i_{xd} + b_4 e_1 e_3 + b_4 i_{xd} e_3 \\
&\quad + b_4 \omega_d e_1 + b_4 i_{xd} \omega_d - di_{yd} + b_0 u_y \\
\dot{e}_3 &= -c_1 e_3 - c_1 \omega_d + c_2 e_1^2 + c_2 i_{xd}^2 + 2c_2 i_{xd} e_1 \\
&\quad + c_3 e_2^2 + c_3 i_{yd}^2 + 2c_3 i_{yd} e_2 + c_4 e_1 e_2 \\
&\quad + c_4 i_{yd} e_1 + c_4 i_{xd} e_2 + c_4 i_{xd} i_{yd} \\
&= -c_1 e_3 + c_2 e_1^2 + 2c_2 i_{xd} e_1 + c_3 e_2^2 + 2c_3 i_{yd} e_2 \\
&\quad + c_4 e_1 e_2 + c_4 i_{yd} e_1 + c_4 i_{xd} e_2.
\end{aligned} \tag{12}$$

3. DESIGN OF THE PROPOSED SPEED CONTROLLER

This section proposes a speed controller for the SRM modeled in the previous section.

Let k_1, k_2, W_1, and W_2 be positive scalars; these scalars are design parameters.

Proposition 1. *The controllers u_x and u_y such that*

$$\begin{aligned}
u_x &= \frac{1}{a_0}\Big(a_1 i_{xd} + a_2 e_1 e_3 + a_2 i_{xd} e_3 + a_2 \omega_d e_1 + a_2 i_{xd} \omega_d - a_3 e_2 \\
&\quad - a_3 i_{yd} - a_4 e_2 e_3 - a_4 i_{yd} e_3 + di_{xd} - a_4 \omega_d e_2 \\
&\quad - a_4 i_{yd} \omega_d - c_2 e_1 e_3 - 2c_2 i_{xd} e_3 - c_4 i_{yd} e_3 - \frac{1}{2} c_4 e_2 e_3 \\
&\quad - k_1 e_1 - W_1 \operatorname{sign} e_1 - k_3 e_2 e_3\Big), \\
u_y &= \frac{1}{b_0}\Big(b_1 i_{yd} + b_2 e_2 e_3 + b_2 i_{yd} e_3 + b_2 \omega_d e_2 + b_2 i_{yd} \omega_d - b_3 e_1 \\
&\quad - b_3 i_{xd} - b_4 e_1 e_3 - b_4 i_{xd} e_3 + di_{yd} - b_4 \omega_d e_1 \\
&\quad - b_4 i_{xd} \omega_d - c_3 e_2 e_3 - 2c_3 i_{yd} e_3 - c_4 i_{xd} e_3 - \frac{1}{2} c_4 e_1 e_3 \\
&\quad - k_2 e_2 - W_2 \operatorname{sign} e_2 - k_3 e_1 e_3\Big)
\end{aligned} \tag{13}$$

guarantee the asympyotic stability of the closed loop system.

Proof. Consider the following Lyapunov function candidate:

$$V_1 = \frac{1}{2} e_1^2 + \frac{1}{2} e_2^2 + \frac{1}{2} e_3^2; \tag{14}$$

Table 1: Parameters of the SRM.

Parameter	Value
Number of phases	4
Number of stator poles	8
Number of rotor poles	6
Stator pole arc	16°
Rotor pole arc	18°
Phase resistance	1.6 Ω
Rated torque	0.4 Nm

taking the deivation of V_1 with respect to time and using (12) and (13), one obtains that

$$\begin{aligned}
\dot{V}_1 &= e_1 \dot{e}_1 + e_2 \dot{e}_2 + e_3 \dot{e}_3 \\
&= -a_1 e_1^2 - a_1 i_{xd} e_1 - a_2 e_1^2 e_3 - a_2 i_{xd} e_1 e_3 - a_2 \omega_d e_1^2 \\
&\quad - a_2 i_{xd} \omega_d e_1 - di_{xd} e_1 + a_3 e_1 e_2 + a_3 i_{yd} e_1 + a_4 e_1 e_2 e_3 \\
&\quad + a_4 i_{yd} e_1 e_3 + a_4 \omega_d e_1 e_2 + a_4 i_{yd} \omega_d e_1 + a_0 e_1 u_x \\
&\quad - b_1 e_2^2 - b_1 i_{yd} e_2 - b_2 e_2^2 e_3 - b_2 i_{yd} e_2 e_3 - b_2 \omega_d e_2^2 \\
&\quad - b_2 i_{yd} \omega_d e_2 - di_{yd} e_2 + b_3 e_1 e_2 + b_3 i_{xd} e_2 + b_4 e_1 e_2 e_3 \\
&\quad + b_4 i_{xd} e_2 e_3 + b_4 \omega_d e_1 e_2 + b_4 i_{xd} \omega_d e_2 + b_0 e_2 u_y \\
&\quad - c_1 e_3^2 + c_2 e_1^2 e_3 + 2c_2 i_{xd} e_1 e_3 + c_3 e_2^2 e_3 + 2c_3 i_{yd} e_2 e_3 \\
&\quad + c_4 e_1 e_2 e_3 + c_4 i_{yd} e_1 e_3 + c_4 i_{xd} e_2 e_3 \\
&= -a_1 e_1^2 - b_1 e_2^2 - c_1 e_3^2 - k_1 e_1^2 - W_1 e_1 \operatorname{sign}(e_1) \\
&\quad - k_2 e_2^2 - W_2 e_2 \operatorname{sign}(e_2).
\end{aligned} \tag{15}$$

Since V_1 is positive definite and $\dot{V}_1$ is negative definite, it can be concluded that the errors converge asymptotically to zero and hence the closed loop system is asymptotically stable. Therefore, the currents i_x, i_y and the speed ω converge to their desired values. □

Remark 1. Note that in the controllers given by (13), the $\operatorname{sign}(e_1)$ and $\operatorname{sign}(e_2)$ terms are added. The addition of these two terms enable the controllers to change structures. Variable structure control is capable of making a control system robust with respect to system parametric uncertainties and external disturbances [25, 26].

4. SIMULATION RESULTS

Simulations of the proposed controller when it is applied to the SRM drive are carried out using MATLAB. The parameters of the motor used for the simulation studies are given

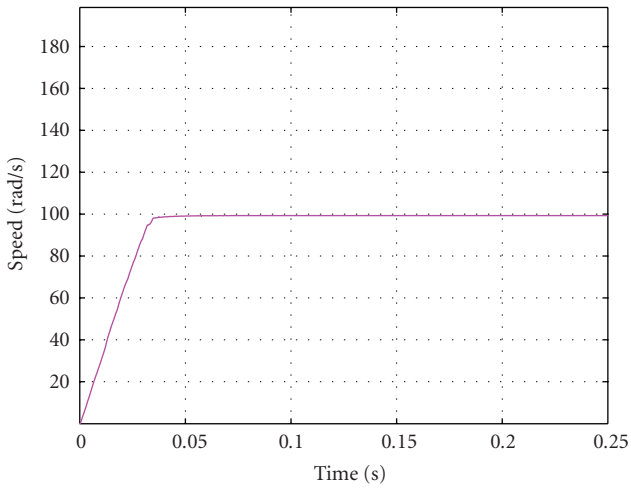

Figure 5: Speed response of the SRM drive.

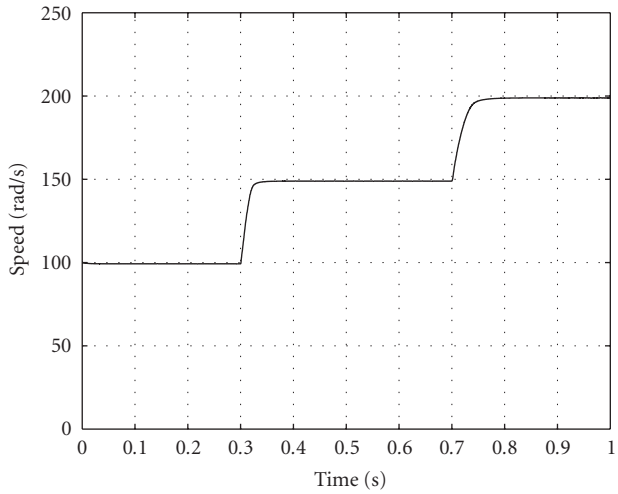

Figure 6: Speed response of the SRM drive.

in Table 1. The excitation angles (θ_{on} and θ_{off}) are kept fixed throughout the simulation studies at 0° and 30°, respectively (note that 0° and 60° correspond to the aligned and the unaligned positions). Two phases are allowed to be excited at one time.

The proposed control scheme needs the measurements of all the states for implementation purposes. The control scheme decides which phases are to be excited at any given instant of time based on rotor position information. High-resolution position encoders are often used to provide the rotor information, and quadrature encoding is used to boost the resolution (pulses per revolution). These encoders are not sensitive to noise. Hall effect sensors are often used to sense the motor phase currents.

For simulation studies, no precautions are needed to increase the drive EMI noise immunity. However, precautions should be taken in real life to protect the power inverter and increase the gate drive circuit EMI noise immunity.

The results of the simulations are presented in the following subsections.

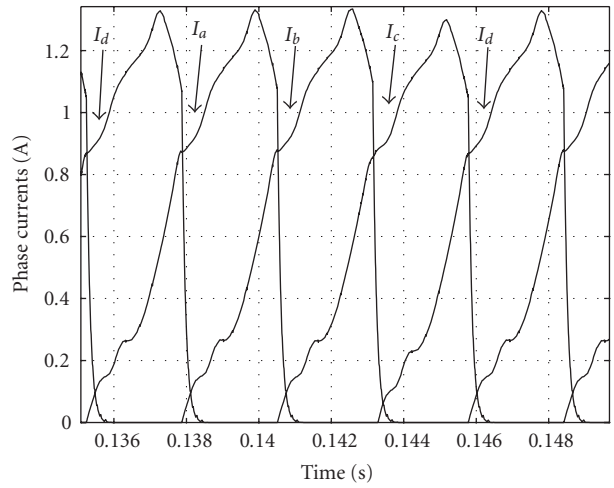

Figure 7: Phase currents waveform of the SRM drive.

4.1. Performance of the system when the developed controller is used

The control law described by (13) is applied to the SRM system described in Section 2. Figure 5 shows the speed response when the motor is commanded to accelerate from rest to a desired speed of 100 rad/s with a load torque of 0.15 Nm. The speed response of the motor when it is allowed to accelerate from rest to a speed of 100 rad/s, then to a speed of 150 rad/s, and finally to a speed of 200 rad/s with a load torque of 0.2 Nm is depicted in Figure 6. It can be seen from the figures that the motor speed converges to the desired speed with a very small steady-state error. It should be mentioned that the ripples in the speed response is due to the sequential switching between the phases and it is not caused by the controller. For completeness, the SRM phase currents waveforms are shown in Figure 7.

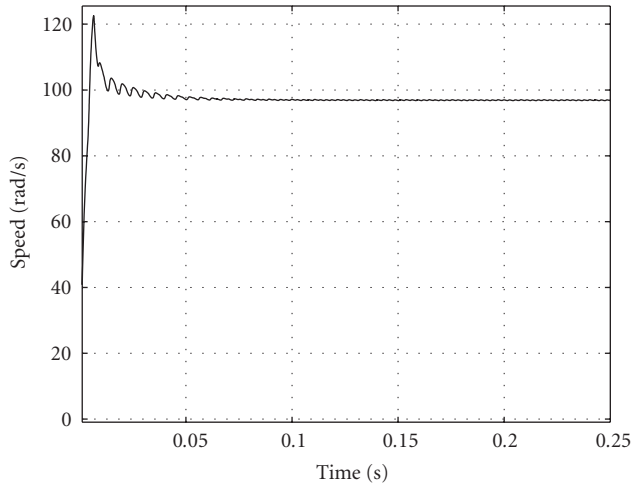

Figure 8: Speed response of the SRM drive when the PI controller is used.

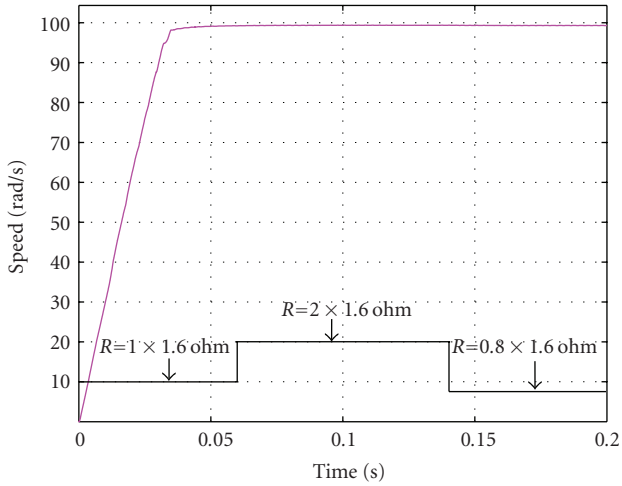

Figure 9: Speed response of the SRM drive with changes in R.

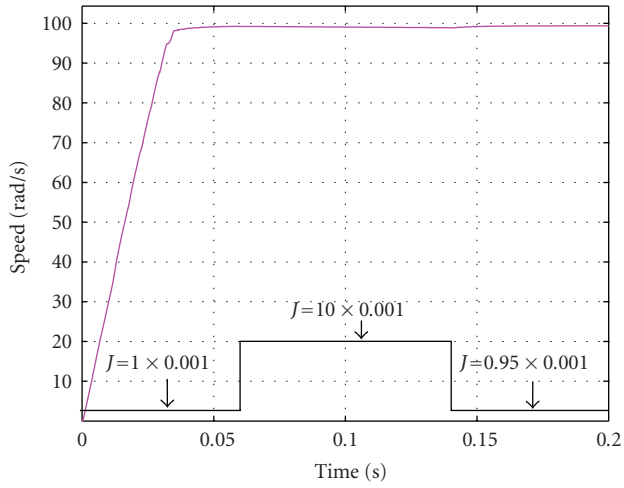

Figure 10: Speed response of the SRM drive with changes in J.

4.2. Performance of the system when PI controller is used

The PI control law

$$u = k_P \omega_{er} + k_I \int \omega_{er}\, dt \tag{16}$$

is used for simulation studies. The PI controller is applied to the SRM drive system described in Section 2. Because the state variables of the SRM drive are highly nonlinearly coupled, the conventional pole-placement method is not suitable in designing a PI controller for the SRM. The gains k_P and k_I are tuned for low-speed and low-load torque operations using trial-and-error method. Figure 8 shows the speed response when the motor is commanded to accelerate from rest to a desired speed of 100 rad/s with a load torque of 0.15 Nm. It can be seen from the figure that the motor speed converges to the desired speed with some overshoot and a small steady state error. The simulation results show that the proposed nonlinear controller yields a better performance than the typical PI controller. Moreover, as discussed in [27], the PI controller requires manual tuning. The PI controller needs to be retuned when the speed command changes. It should be mentioned that the gains used for simulation studies are obtained after several trials.

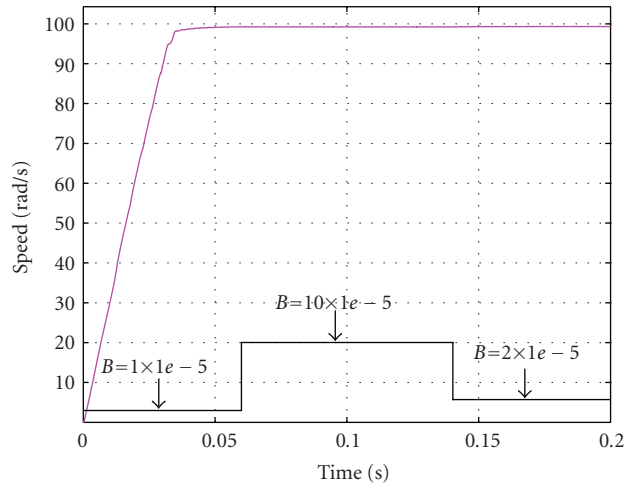

Figure 11: Speed response of the SRM drive with changes in B.

4.3. Robustness of the proposed control scheme

Simulation studies are undertaken to test the robustness of the proposed controllers to changes in the parameters of the SRM and changes in the load torque. Changes in the phase resistance R, the rotor inertia J, and the damping factor B are investigated through simulations. The simulations are carried out by step changing one parameter at one time while keeping all the other parameters unchanged. The motor is commanded to accelerate from rest to a desired speed of 100 rad/s with a load torque of 0.15 Nm. Step changes in one of the parameters of the motor occur at time $t = 0.06$ s and at time $t = 0.14$ s.

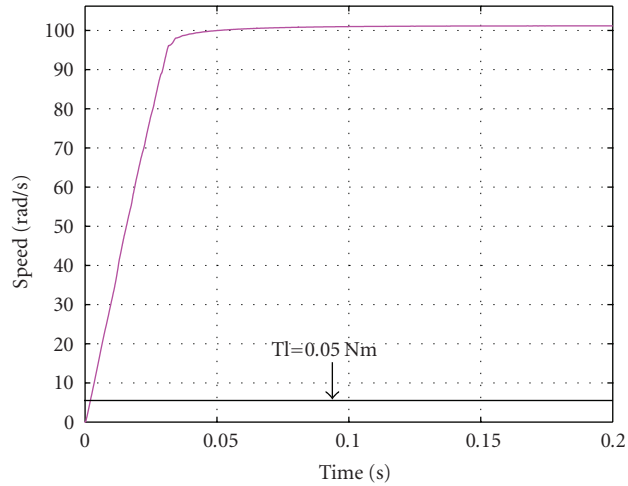

Figure 12: Speed response of the SRM drive with load torque 0.05 Nm.

Figures 9–11 show the motor responses when there are changes in the parameters of the SRM system. Figure 9 shows the response of the motor when the phase resistance is increased by 100% of its original value and then decreased by 20% of its original value. Figure 10 shows the response of the motor when the rotor inertia is varied by up to 10 times its original value. Figure 11 shows the response of the motor when the damping factor B is varied by up to 10 times its original value. It is clear from the figures that the speed responses of the motor converge to the desired speed even when the parameters of the system change drastically. Hence, it can be concluded that the simulation results show that the proposed controller is robust to changes in the parameters of the SRM system.

It is desirable for high-performance applications that the proposed control scheme be robust to variations in the load torque. Simulation studies are carried out to demonstrate the robustness of the proposed controller to changes in the load torque. The motor is commanded to accelerate from rest to a desired speed of 100 rad/s. Figures 12–14 show the motor responses when the load torque takes on the values of 0.05, 0.1, and 0.15 Nm, respectively. Figure 12 shows the motor response when the load torque is 0.05 Nm. Figure 13 shows the motor response when the load torque equals 0.1 Nm. Figure 14 shows the motor response when the load torque equals 0.15 Nm. It can be seen that the speed response converges to its desired value for the different values of the load torque. Figure 15 depicts the motor response when the load torque changes during the motion of the rotor. The load torque is originally 0.15 Nm, then it briefly becomes 0.4 Nm, and then it changes back to its original value. It can be seen from the figure that the motor speed response shows a small dip in the speed when the load is suddenly changed, however the controller is able to keep the motor speed very close to the desired speed.

Therefore, it can be concluded from the simulation studies that the proposed nonlinear controller is robust to changes in the parameters of the SRM system and to changes in the load torque.

For comparison purposes, the output torque at low speed of 10 rad/s (around 100 rpm) is shown in Figure 16 when the mutual inductance is neglected; the output torque is shown in Figure 17 when the mutual inductance is considered. It can be seen from these figures that the proposed control scheme has to some extent reduced the torque ripples when the mutual inductance is taken into account. It should be noted that the overall system performance is determined by the characteristics of the machine, the power converter, and the controller. Torque ripples at very low speed are an important factor in characterizing position control. However, for speed control, small torque ripples at high speeds are usually accepted given that the motor speed follows the desired speed.

5. CONCLUSION

The design of a nonlinear controller for speed regulation applications for an SRM has been presented in this paper.

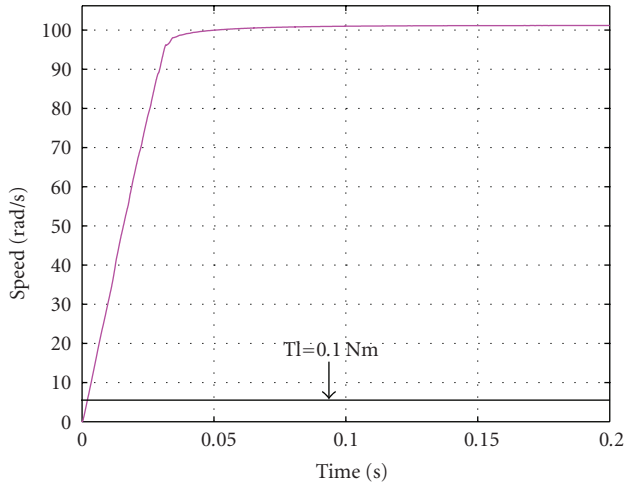

Figure 13: Speed response of the SRM drive with the load torque 0.1 Nm.

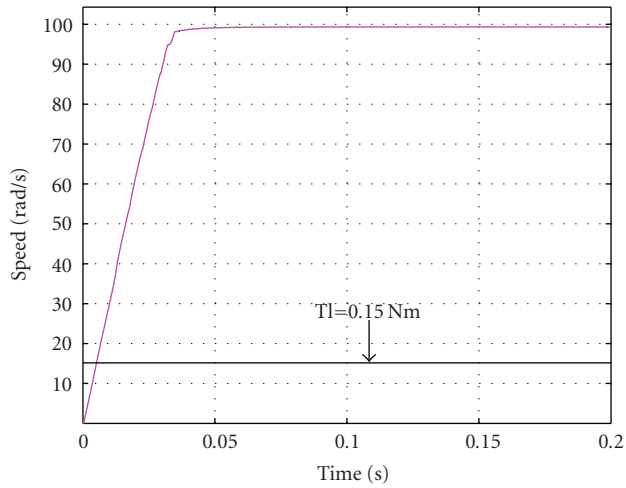

Figure 14: Speed response of the SRM drive with load torque 0.15 Nm.

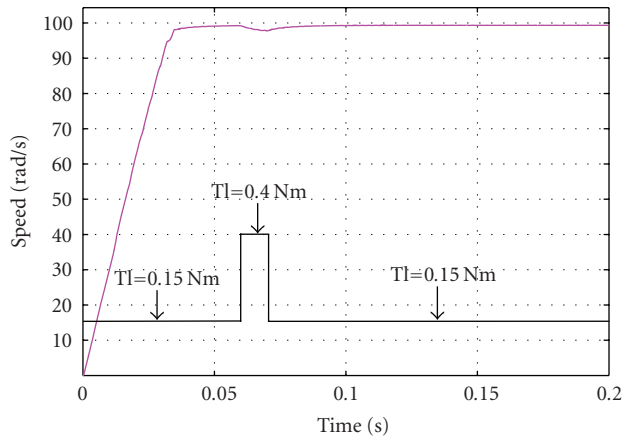

Figure 15: Speed response of the SRM drive with changes in the load torque.

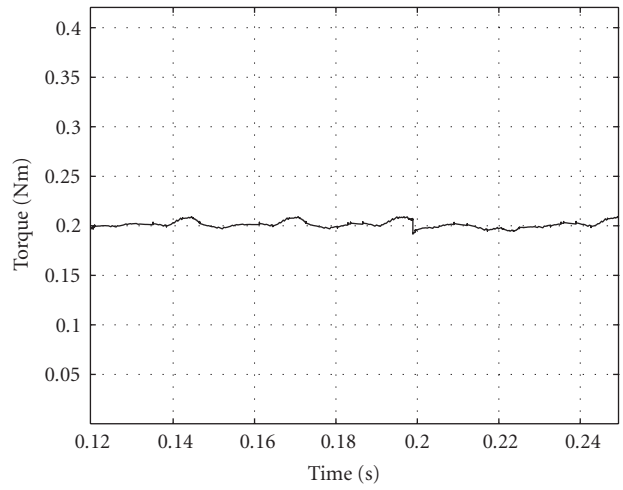

Figure 16: Output torque of the SRM drive with mutual inductance neglected (load torque 0.2 Nm and speed 10 rad/s).

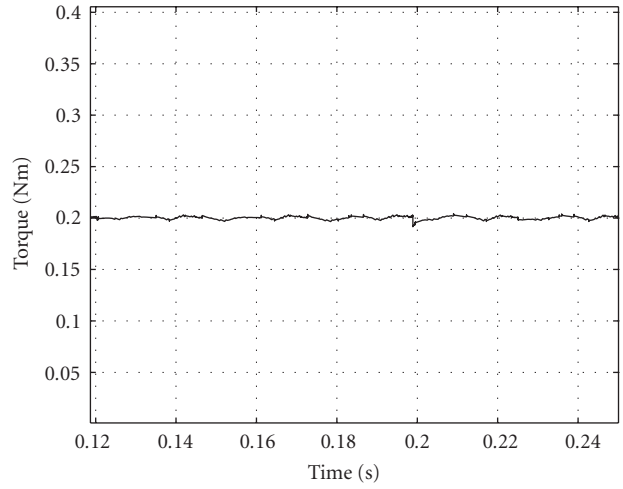

Figure 17: Output torque of the SRM drive with mutual inductance considered (load torque 0.2 Nm and speed 10 rad/s).

An SRM model which includes the effects of mutual inductances and which is suitable for two-phase excitation has been adopted. Experimentally verified SRM parameters which takes mutual effects into account were used for the simulation studies.

Simulation results show that the proposed nonlinear control scheme works well. The controller reduces the torque ripples and compensates the effect of mutual inductance. Moreover, the simulation results indicate that the proposed control scheme is robust to changes in the parameters of the system; and robust to variations in the load torque.

Future work will address the extension of the proposed control algorithm to include the nonlinear operational region, and the implementation of the proposed control scheme using a DSP-based digital controller board and a hardware setup.

REFERENCES

[1] T. J. E. Miller, *Switched Reluctance Motors and Their Control*, Clarendon Press, Oxford, UK, 1993.

[2] R. Krishnan, *Switched Reluctance Motor Drives*, CRC Press, Cambridge, UK, 2001.

[3] P. J. Lawrenson, J. M. Stephenson, P. T. Blenkinsop, J. Corda, and N. N. Fulton, "Variable-speed switched reluctance motor," *IEE Proceedings B*, vol. 127, no. 4, pp. 253–265, 1980.

[4] D. S. Schramm, B. W. Williams, and T. C. Gaeen, "Torque ripple reduction of switched reluctance motors by phase current optimal profiling," in *Proceedings of the 23rd Annual IEEE Power Electronics Specialist Conference (PESC '92)*, pp. 857–860, Toledo, Spain, June-July 1992.

[5] I. Husain and M. Ehsani, "Torque ripple minimization in switched reluctance motor drives by PWM current control," *IEEE Transactions on Power Electronics*, vol. 11, no. 1, pp. 83–88, 1996.

[6] M. Ilic-Spong, T. J. E. Miller, S. R. MacMinn, and J. S. Thorp, "Instantaneous torque control of electric motor drives," *IEEE Transactions on Power Electronics*, vol. 2, no. 1, pp. 55–61, 1987.

[7] R. S. Wallace and D. G. Taylor, "A balanced commutator for switched reluctance motors to reduce torque ripple," *IEEE Transactions on Power Electronics*, vol. 7, no. 4, pp. 617–626, 1992.

[8] C.-H. Kim and I.-J. Ha, "A new approach to feedback-linearizing control of variable reluctance motors for direct drive applications," *IEEE Transactions on Control Systems Technology*, vol. 4, no. 4, pp. 348–362, 1996.

[9] P. Pillay, Y. Liu, W. Cai, and T. Sebastian, "Multiphase operation of switched reluctance motor drives," in *Proceedings of the IEEE Industry Applications Conference (IAS '97)*, vol. 1, pp. 310–317, New Orleans, La, USA, October 1997.

[10] J. C. Moreira and T. A. Lipo, "Simulation of a four phase switched reluctance motor including the effects of mutual coupling," *Electric Machines and Power Systems*, vol. 16, no. 4, pp. 281–299, 1989.

[11] P. P. De Paula, W. M. Da Silva, J. R. Cardoso, and S. I. Nabeta, "Assessment of the influences of the mutual inductances on switched reluctance machines performance," in *Proceedings of the IEEE International Electric Machines and Drives Conference (IEMDC '03)*, vol. 3, pp. 1732–1738, Madison, Wis, USA, June 2003.

[12] M. Krishnamurthy, B. Fahimi, and C. S. Edrington, "On the measurement of mutual inductance for a switched reluctance machine," in *Proceedings of the 37th IEEE Power Electronics Specialists Conference (PESC'06)*, pp. 1–7, Jeju, Korea, June 2006.

[13] J.-W. Ahn, S.-G. Oh, J.-W. Moon, and Y.-M. Hwang, "A three-phase switched reluctance motor with two-phase excitation," *IEEE Transactions on Industry Applications*, vol. 35, no. 5, pp. 1067–1075, 1999.

[14] H. H. Moghbelli, G. E. Adams, and R. G. Hoft, "Prediction of the instantaneous and steady state torque of the switched reluctance motor using FEM with experimental results comparison," *Electric Machines and Power Systems*, vol. 19, no. 3, pp. 287–302, 1991.

[15] H.-K. Bae and R. Krishnan, "A novel approach to control of switched reluctance motors considering mutual inductance," in *Proceedings of the 26th Annual Conference of the Industrial Electronics Society (IECON '00)*, vol. 1, pp. 369–374, Nagoya, Japan, October 2000.

[16] H.-K. Bae, B.-S. Lee, P. Vijayraghavan, and R. Krishnan, "A linear switched reluctance motor: converter and control," *IEEE*

Transactions on Industry Applications, vol. 36, no. 5, pp. 1351–1359, 2000.

[17] B.-S. Lee, H.-K. Bae, P. Vijayraghavan, and R. Krishnan, "Design of a linear switched reluctance machine," *IEEE Transactions on Industry Applications*, vol. 36, no. 6, pp. 1571–1580, 2000.

[18] R. Krishnan and P. Materu, "Measurement and instrumentation of a switched reluctance motor," in *Proceedings of the IEEE Industry Applications Society Annual Meeting (IAS '89)*, vol. 1, pp. 116–121, San Diego, Calif, USA, October 1989.

[19] H. K. Bae and R. Krishnan, "A study of current controllers and development of a novel current controller for high performance SRM drives," in *Proceedings of the 31st IEEE Industry Applications Society Annual Meeting (IAS '96)*, vol. 1, pp. 68–75, San Diego, Calif, USA, October 1996.

[20] C. W. Trowbridge, *An Introduction to Computer Aided Electromagnetic Analysis*, Vector Fields, Oxford, UK, 1990.

[21] A. R. Eastham, H. Yuan, G. E. Dawson, P. C. Choudhury, and P. M. Cusack, "A Finite element evaluation of pole shaping in switched reluctance motors," *Electrosoft*, vol. 1, no. 1, pp. 55–67, 1990.

[22] G. E. Dawson, A. R. Eastham, and J. Mizia, "Switched - reluctance motor torque characteristics: finite-element analysis and test results," *IEEE Transactions on Industry Applications*, vol. 23, no. 3, pp. 532–537, 1987.

[23] J. F. Lindsay, R. Arumugam, and R. Krishnan, "Finite-element analysis characterization of a switched reluctance motor with multitooth per stator pole," *IEE Proceedings B*, vol. 133, no. 6, pp. 347–353, 1986.

[24] R. Arumugam, D. A. Lowther, R. Krishnan, and J. F. Lindsay, "Magnetic field analysis of a switched reluctance motor using a two-dimensional finite element model," *IEEE Transactions on Magnetics*, vol. 21, no. 5, pp. 1883–1885, 1985.

[25] F. M. Al-Sunni and S. K. Mukarram, "An adaptive variable structure controller for linearizable systems," *Journal of King Abdulaziz University Engineering Science*, vol. 14, no. 1, pp. 65–76, 2002.

[26] R. A. Decarlo, S. H. Zak, and G. P. Matthews, "Variable structure control of nonlinear multivariable systems: a tutorial," *Proceedings of the IEEE*, vol. 76, no. 3, pp. 212–232, 1988.

[27] N. Inanc and V. Ozbulur, "Torque ripple minimization of a switched reluctance motor by using continuous sliding mode control technique," *Electric Power Systems Research*, vol. 66, no. 3, pp. 241–251, 2003.